Few-boson tunneling dynamics of strongly correlated binary mixtures in a double well

Budhaditya Chatterjee,[*] Ioannis Brouzos,[†] Lushuai Cao,[‡] and Peter Schmelcher[§]
Zentrum für Optische Quantentechnologien, Universität Hamburg, Luruper Chaussee 149, D-22761 Hamburg, Germany
(Received 19 May 2011; published 5 January 2012)

We explore the tunneling dynamics of strongly correlated bosonic mixtures in a one-dimensional double well. The roles of the inter- and intraspecies interactions and their interplay are investigated using the numerically exact multiconfiguration time-dependent Hartree (MCTDH) method. The dynamics is studied for three initial configurations: complete and partial population imbalance and a species-separated state. Increasing the interspecies interaction leads to a strong increase of the tunneling time period analogous to the quantum self-trapping for condensates. The intraspecies repulsion can suppress or enhance the tunneling period depending on the strength of the interspecies correlations as well as the initial configuration. Completely correlated tunneling between the two species and within the same species as well as mechanisms of species separation and counterflow are revealed. These effects are explained by studying the few-body energy spectra as well as the properties of the contributing stationary states.

DOI: 10.1103/PhysRevA.85.013611 PACS number(s): 67.85.−d, 67.60.Bc, 05.30.Jp

I. INTRODUCTION

Ultracold atoms represents a distinct phase of matter for the exploration of fundamental quantum processes [1–3]. The ability to precisely control ultracold systems has triggered investigations in different fields such as quantum simulation and information processing [4], quantum phase transitions [5,6], and driven quantum systems [7]. Experimentally it is possible to control not only the external potentials but also the effective interactions between the atoms using Feshbach resonances [8]. Moreover, dimensionality can be tuned, and in particular quasi-one-dimensional systems can be achieved by confining two transverse degrees of freedom. In such waveguide-like systems, confinement-induced resonances [9] provide an additional tool to tune the interactions, thus making the study of strongly correlated systems experimentally feasible. An interesting observation for a single-species bosonic system in one dimension is that infinitely strongly repulsively interacting bosons possess the same local properties as a system of noninteracting fermions. This effect, known as fermionization, has been experimentally observed [10,11] and can be explained via Bose-Fermi mapping [12].

Inspired by the results of single bosonic species, recently there has been a lot of experimental [13–17] and theoretical [18–28] interest in the static properties of multispecies bosonic mixtures. In these systems, the interplay between the inter- and intraspecies forces as well as different masses or potential asymmetry give rise to various phenomena and effects not accessible in the single-component case. For instance, the process of composite fermionization occurs when the interspecies coupling is set to infinity and the strong repulsion provides different pathways for phase separation [19,20,24]. Moreover, instabilities [18] as well as new phases such as paired and counterflow superfluidity [28] have been observed.

Focusing on the quantum dynamics, the double well provides the simplest prototype for a finite lattice and Josephson junction and is especially a very elucidating case for studying the fundamental characteristics of quantum tunneling. Theoretically, the tunneling dynamics of single species through the crossover from weak to strong interaction regimes reveal interesting effects such as Josephson oscillations, pair tunneling, self-trapping, and fermionization [29–33], which have also been observed experimentally [34,35].

More recently, these studies have been extended also to systems of binary bosonic mixtures [36–43]. These works demonstrate various effects such as macroscopic quantum self-trapping and coherent quantum tunneling [36], observations of collapse and revival of population dynamics [41,42], symmetry breaking and restoring scenarios [39], as well as dipole-oscillation-induced pairing and counterflow superfluidity [43].

However, most of the work has been done on the mean-field level either by solving Gross-Pitaevskii equations or by using the lowest band Bose-Hubbard model. Although these studies do provide interesting insights into the mechanism of tunneling, an investigation of the complete crossover from the weak to strong interaction regime allows the examination of new effects and mechanisms not present, for example, in the mean-field description. For instance, referring to the case of two species in a harmonic trap, it has been found that if one species is localized due to its heavy mass, then it can act as an effective material barrier through which the lighter component tunnels [44,45]. The feedback of this material barrier leads to different pairing mechanisms for the light species. Moreover, few-body systems provide a bottom-up approach toward the understanding of many-body phenomena. Experiments exploring few-atom systems in finite optical lattices [46] serve as promising setups for designing transistor-like structures from the perspective of atomtronics.

In this paper, we study the tunneling dynamics of a binary mixture of bosonic species in a one-dimensional double well from a few-body perspective. Using the numerically exact multiconfiguration time-dependent Hartree (MCTDH) method (see Appendix) [47,48], we investigate the crossover from weak to strong interactions, focusing in particular on microscopic quantum effects and mechanisms which are prominent in few-body systems. We demonstrate how the

[*]bchatter@physnet.uni-hamburg.de
[†]ibrouzos@physnet.uni-hamburg.de
[‡]lcao@physnet.uni-hamburg.de
[§]pschmelc@physnet.uni-hamburg.de

interplay between the inter- and intraspecies interactions affect the rate and behavior of the tunneling in a nontrivial way. A strong increase of the tunneling period is observed as the interspecies repulsion is increased. However, in certain cases and especially for the strongly interacting regime, increasing the intraspecies interactions leads to an increase of the tunneling rates, in contrast to what is observed for single-species systems. Preparing different initial states leads consequently to diverse tunneling behavior. For complete imbalance of the populations, that is, when the particles are all prepared initially in the same well or when the species are localized at different wells (species separation), the tunneling is strongly correlated, meaning that the species tunnel either in phase or out of phase. Only for very strong intraspecies interactions are these correlations reduced. On the other hand, for partial population imbalance (e.g., one species is delocalized and the second one is localized), a mechanism of species separation and counterflow appears. The various effects are attributed to the features of the energy spectrum and explained by examining the density profile of the contributing stationary states.

The paper is organized as follows. In Sec. II, we introduce our model and setup. Subsequently, we present and discuss the results for the quantum dynamics of the mixture with three bosons (two bosons of species A and one of species B). Three initial-state scenarios are examined: complete population imbalance in Sec. III, complete species separation in Sec. IV, and partial imbalance in Sec. V. The computational method MCTDH is described in Appendix.

II. MODEL AND SETUP

We consider a mixture of two species of bosons labeled by A and B in a one-dimensional double-well potential. These may correspond to two different kinds of atoms or could be two hyperfine states of the same atomic species. The fact that there are two different species induces distinguishability and thus fundamentally alters the physics and in particular the quantum dynamics compared to the case of a single species.

Our Hamiltonian reads (see [24] for details)

$$H = \sum_{\sigma=A,B}\sum_{i=1}^{N_\sigma}\left[\frac{p_{\sigma,i}^2}{2M_\sigma} + U_\sigma(x_{\sigma,i}) + \sum_{i<j} V_\sigma(x_{\sigma,i}-x_{\sigma,j})\right] + \sum_{i=1}^{N_A}\sum_{j=1}^{N_B} V_{AB}(x_{A,i}-x_{B,j}), \quad (1)$$

where $M_{A,B}$ is the mass for species A and B, respectively.

We assume here that the different species obey the same single-particle Hamiltonian, that is, they possess the same mass and experience the same single-particle potential. The double-well potential $U(x) = \frac{1}{2}M\omega x^2 + h\delta_\omega(x)$ is modeled as a harmonic potential with a central barrier shaped as a Gaussian $h\delta_\omega(x) = h\frac{e^{-x^2/2s^2}}{\sqrt{2\pi}s}$ of width $s = 0.5$ and height $h = 8.0$. Dimensionless harmonic-oscillator units, that is, $M_A = M_B = 1$, $\omega = 1$, are employed throughout. In the ultracold scattering limit, one can approximate the interaction (both intra-V_σ and interspecies V_{AB}) with an effective contact potential [9]:

$$V_\sigma(x_{\sigma,i}-x_{\sigma,j}) = g_\sigma\delta(x_{\sigma,i}-x_{\sigma,j}),$$
$$V_{AB}(x_{A,i}-x_{B,j}) = g_{AB}\delta(x_{A,i}-x_{B,j}).$$

Numerically, we sample the δ function as a very narrow Gaussian (choosing, of course, a spatial grid dense enough to sample this narrow peak).

The different initial configurations are achieved by adding a tilt to the double well, which can be different for the two species depending on the required state. Thus, an individual well could be made energetically more favorable (tilted) for a certain species. For instance, to prepare a complete imbalance, the double wells of both species are tilted the same way, while to prepare a species-separated scenario, U_A is tilted opposite to U_B. To prepare the partial population imbalanced state, one has to tune the tilt for both species judiciously depending on the given interaction strength such that the required population configuration is achieved. The ground state is then computed by the relaxation method and results in the desired initial state. For the study of the dynamics, the tilt is instantaneously ramped down to obtain a symmetric double well at $t = 0$.

In order to investigate systematically and in detail the tunneling processes for binary mixtures, we consider the simplest nontrivial few-body system consisting of two bosons of species A and one of species B. This system captures the most important microscopic quantum dynamical processes occurring for few-body bosonic mixtures. In this case, we have two independent parameters g_{AB} and g_A (since there is only a single boson B species). When the interspecies interaction g_{AB} is zero, the two components are completely decoupled, meaning that the single B boson will undergo Rabi oscillations between the wells. The A bosons will then follow a correlated two-particle dynamics regulated by the intraspecies interaction g_A. (This case is not addressed here but has been discussed in detail in the literature [32,33].) Another case which reduces to that of a single species is $g_{AB} \to g_A$, where the essentials of the tunneling dynamics are those of three particles of a single species. Our focus is exclusively on the cases where we expect significant deviations from the single-species scenario.

III. COMPLETE POPULATION IMBALANCE

We begin our study by exploring the quantum dynamics for an initial state where all the atoms are loaded into the left well. As observables, we compute the time evolution of the one-particle density of each species and the resulting population in each well. For the right well, we have

$$n_\alpha(t) = N_\alpha\int_0^\infty \rho_\alpha(x;t)dx, \quad (2)$$

where ρ_α is the one-body density of the species $\alpha = A, B$ and the total population of the right well is $n_R = n_A + n_B$. Due to symmetry and resonant mechanisms, we always have a complete transfer of the population of both species between the two wells, which happens in most cases according to a periodic pattern with period T.

1. *Repulsive interspecies interaction and binding mechanisms*

The most important effect of increasing the interspecies interaction g_{AB} is a very strong increase of the tunneling

TABLE I. Tunneling periods for different g_{AB} values for the case of complete imbalance.

Period	$g_{AB} = 0.0$	$g_{AB} = 0.2$	$g_{AB} = 5.0$	$g_{AB} = 25.0$
$g_A = 0.0$	2×10^2	1×10^3	9×10^3	1×10^6
$g_A = 0.2$	6×10^2	6×10^3	1×10^4	1×10^6

period up to very large values. This can be seen in Table I, where we show the tunneling period with increasing g_{AB}. This behavior is counterintuitive since with increasing repulsion between the species initially localized in the same well one would expect the tunneling to be enhanced. The delayed tunneling is reminiscent of the one found for the case of a single species [24,33] and is the few-body equivalent of self-trapping. The primary reason for this decrease of the tunneling frequency, especially for low interactions (within the so-called Bose-Hubbard regime), can be attributed to the energy spectrum presented in Fig. 1 considering the states that contribute to the dynamics. The eigenstates are typically characterized by the superpositions of different number states such as $|AA,B\rangle$, where the vector indicates two A boson occupying the left well and one B boson in the right well. As g_{AB} increases, different doublets are formed in this lowest band. The energetically highest doublet shown in Fig. 1, consisting primarily of the states $|AAB,0\rangle \pm |0,AAB\rangle$, is of relevance to our case since these eigenstates possess maximum overlap with our initial state $|AAB,0\rangle$.

With increasing g_{AB}, the number states $|AAB,0\rangle$ and $|0,AAB\rangle$ depart energetically from other number states due to their big on-site interaction energy (having all bosons in the same well) and the eigenstates $|AAB,0\rangle \pm |0,AAB\rangle$ become increasingly degenerate, thereby forming a doublet. The tunneling then consists of oscillations between $|AAB,0\rangle$ and $|0,AAB\rangle$, while the decreasing energy splitting of the doublet leads to an increase of the tunneling period. This is the few-body analog of the self-trapping mechanism in single-species condensates. The impressive fact is that this behavior is even more pronounced for higher interactions (see, e.g., $g_{AB} = 5.0,25.0$ in Table I), in contrast to the single-species case (see [24,33]) where there is a reduction of the period

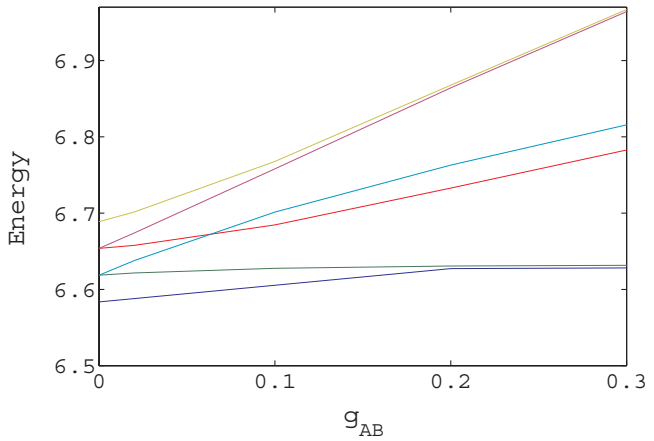

FIG. 1. (Color online) Energy spectrum for $g_A = 0.0$ and small interaction strengths g_{AB}.

due to higher band contributions and fermionization (with the particles tunneling as uncorrelated fermionized bosons with the corresponding Rabi frequency) in the strong interaction limit. In our case, as long as the interaction takes place predominantly between the different species (here for simplicity $g_A = 0$), first there is no fermionization in the regular sense and second the particles tunnel in a highly correlated manner, meaning that the initial localized state $|AAB,0\rangle$ does not tunnel to states like $|B,AA\rangle$ or $|AB,A\rangle$ since they possess much lower interaction energy and are thus energetically of-resonant. The fact that we encounter correlated particle tunneling (all bosons together) is documented by the probability of finding all the particles in the same well, which remains very close to unity throughout the dynamics. As a first conclusion, we see that the repulsive interspecies interaction causes "binding" between the particles and reduces the tunneling rates.

2. *Intraspecies interactions to control tunneling and correlations*

In contrast to the one-way effect of the g_{AB} in the tunneling dynamics, the intraspecies repulsion g_A plays a more complicated role, controlling both the tunneling period and the degree of correlations. Let us first explore a weak interspecies interaction strength $g_{AB} = 0.2$. In Fig. 2, we illustrate the tunneling dynamics for different values of g_A at $g_{AB} = 0.2$ for species A and B by showing the population of the right well, n_A,n_B. Except for the periods T of the tunneling envelope, one also observes rapid small-amplitude oscillations. Concerning T, we obtain a monotonic increase as $g_A = 0.0 \to 0.3$. However, this behavior changes as we go beyond the weak interaction regime for g_A and we observe a decrease of the tunneling period for $g_A = 5$. Another important feature is that the two components A and B undergo roughly the same evolution of the oscillation pattern [compare Figs. 2(a) and 2(b)], which is suggestive of strong inter- and intraspecies correlations in the sense that all bosons tunnel together. This changes slightly only for very strong interaction $g_A = 25$, where the tunneling period reduces substantially while the pattern becomes more erratic, consisting of two primary oscillations. Unlike the previous cases, the dynamics of the two components are not completely identical. This indicates, in the line of argumentation provided above, a reduction of the correlations between the two species and attempted single-particle tunneling.

Within the weak interaction regime where the effective lowest band number states description is valid, the tunneling process of shuffling between the two completely localized states $|AAB,0\rangle$ and $|0,AAB\rangle$ can be more specifically described by the sequence $|AAB,0\rangle \to |AB,A\rangle \to |B,AA\rangle \to |0,AAB\rangle$. The effective tunneling rate within this lowest band description is approximately given by

$$f \sim J^3/(E_1 - E_2)(E_1 - E_3), \tag{3}$$

where J is the effective coupling term between the two sites, E_1 is the energy of the initial and final number state of the tunneling, and E_2,E_3 are the energies of the intermediate number states, which in this case are $|AB,A\rangle$ and $|B,AA\rangle$. Considering the interaction part of the number states, the completely localized states $|AAB,0\rangle$ and $|0,AAB\rangle$ have energies $\sim 2g_{AB} + g_A$ while the states $|AB,A\rangle$ and $|B,AA\rangle$

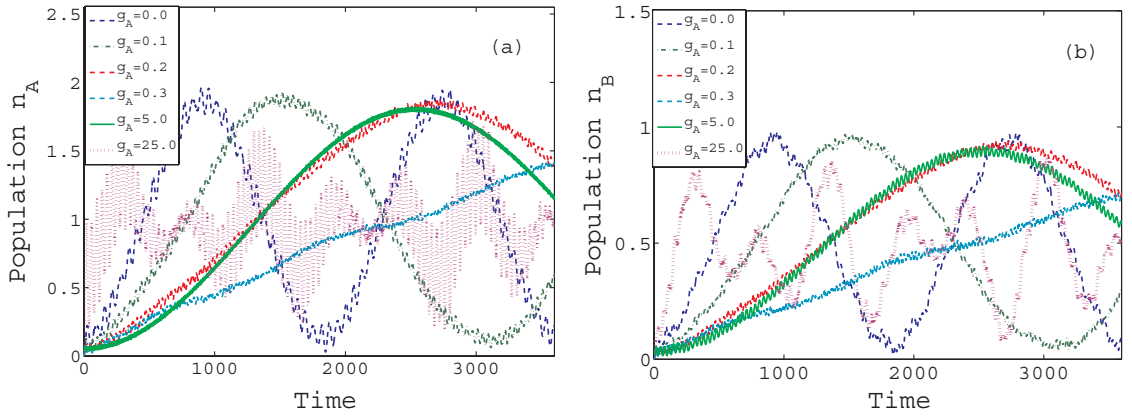

FIG. 2. (Color online) Population of the right well (a) n_A of species A and (b) n_B of species B at $g_{AB} = 0.2$ for different g_A values.

have energies $\sim g_{AB}$ and g_A respectively. Therefore, for this tunneling process, the tunneling rate according to Eq. (3) scales as $f \sim J^3/2g_{AB}(g_{AB} + g_A)$. From this relation, it follows that the tunneling rate decreases for increasing g_A in the weak interaction regime, as we have seen above.

The opposite effect (i.e., decrease of the tunneling period, as g_A increases further beyond the weak coupling regime) is attributed to the increasing splitting of the main contributing doublet $|AAB,0\rangle \pm |0,AAB\rangle$ as g_A increases. Additionally, contributions of higher bands appear, especially for stronger intraspecies interactions $g_A = 25.0$, which breaks the completely correlated tunneling behavior, allowing for attempted single-particle tunneling into energetically higher number states like $|AB,A\rangle$.

Turning now to higher interspecies interaction $g_{AB} = 5.0$, we observe in Fig. 3 that the tunneling period decreases strongly as g_A increases. Since g_{AB} is in this case beyond the weak coupling regime, we focus on an analysis of the density profiles of the contributing eigenstates shown in Fig. 4 to understand the effect of increasing g_A. As g_A increases, the repulsion of the A bosons leads to a broadening of their density profile. This broadening leads to a greater overlap of the wave functions of A atoms localized in the left and the right wells, and this in turn increases the effective tunneling coupling and the corresponding tunneling rates. At $g_A = 0$, the localized densities ρ_A and ρ_B are spatially separated in each well as a consequence of the repulsion between the species. Note that the density of the B boson possesses its maximum for larger values of $|x|$, thereby "sandwiching" the A boson population. This arises from the fact that due to the unequal number ($N_A > N_B$), it is energetically favorable to shift the density of the B species to larger values of $|x|$. As g_A is increased, the two localized densities ρ_A,ρ_B in the two wells gain an increasing overlap, which can be observed as a vertical upward shift of the density profile at $x = 0$ that becomes progressively stronger with increasing g_A. This mechanism, also present for other contributing states, leads to an overall increase of the tunneling coupling and consequently to an increase of the tunneling frequency for strong interactions.

The overall features with respect to the different time scales and oscillatory tunneling behavior is similar for very strong interspecies interactions $g_{AB} = 25.0$ with the exception of $g_A = 20.0$ [Fig. 5(a)]. Only this case can be considered as a tunneling mechanism close to fermionization. In this regime, the bosons become isomorphic with noninteracting fermions, and thus the tunneling dynamics approaches that of independent noninteracting fermions. The latter tunneling frequency is close to the Rabi frequency, which is significantly faster than the previously discussed cases. To understand the reduction of period from a number-state perspective, we note that the nearly fermionized bosons occupy both the lowest band and the first excited band. As a consequence, the previously off-resonant intermediate number states (namely the states $|AAB,0\rangle$, $|AB,A\rangle$, and $|B,AA\rangle$) become near resonant, since the particles can tunnel between the excited band of the two wells without significant change of energy. This results

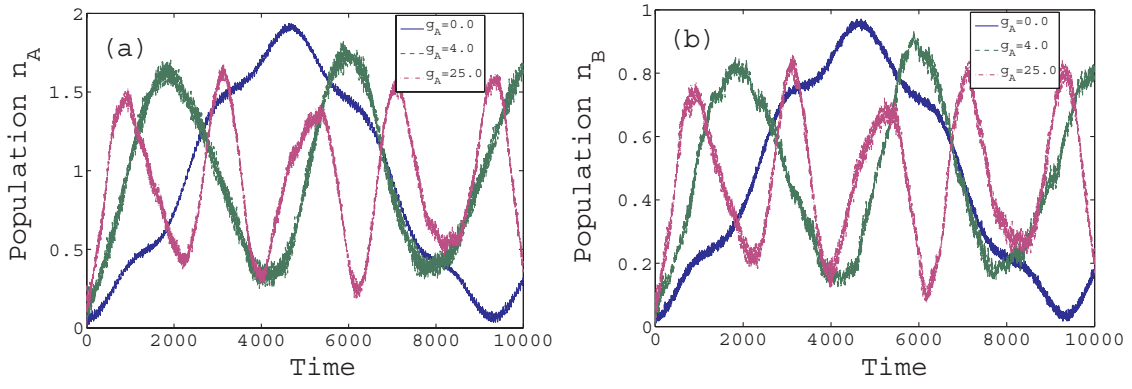

FIG. 3. (Color online) Population in the right well (a) n_A of species A and (b) n_B of species B at $g_{AB} = 5.0$ for different g_A values.

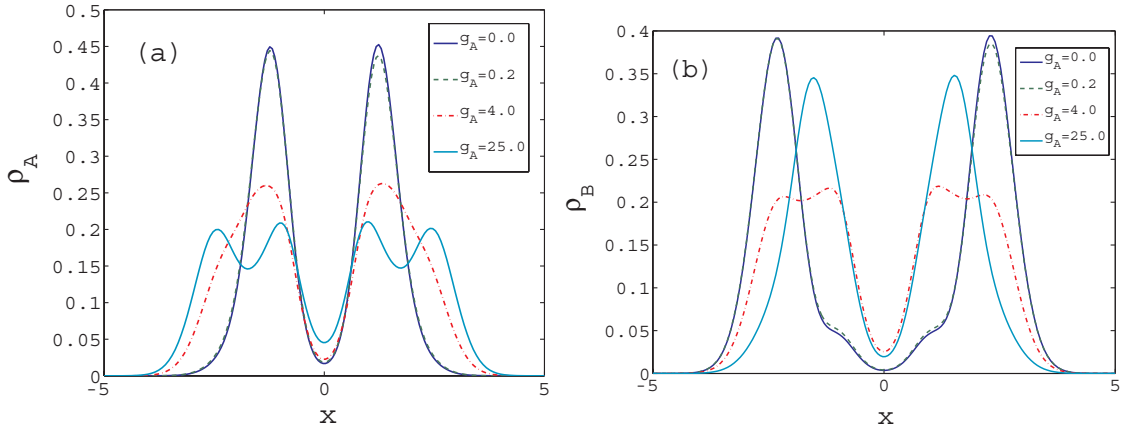

FIG. 4. (Color online) One-particle density as obtained by taking into account the most important eigenstates contributing to the initial state for (a) species A and (b) species B for $g_{AB} = 5.0$.

in a reduction of the effective tunneling period while the separation of the time scales involved in the dynamics is strongly reduced. The correlations among the bosons with respect to the tunneling process are also strongly reduced, as can be seen in Fig. 5(b), where the pair and triple correlations show a strong deviation from the value 1, that is, from the strongly correlated case.

IV. SPECIES-SEPARATED INITIAL STATE

Let us now consider the initial state for which the two species are localized in different wells, the A bosons in the left well and the B boson in the right well. Similar to the previous scenario, increasing g_{AB} leads again to an increase of the tunneling period, an effect which is intuitive here since the components that are initially prepared in different wells are forced to stay apart from each other by the repulsive interspecies force. Moreover, an important point to note is that the contributing states are always those of the lowest band, and the number states mainly involved are $|AA,B\rangle$ and $|B,AA\rangle$ since the former one is the initial state. Therefore, as long as g_A remains comparatively small, the dynamics consists of a slow oscillation between the states $|AA,B\rangle$ and $|B,AA\rangle$ and is correlated in the sense that the A and B bosons always occupy different wells in the course of the dynamics.

This is shown in Figs. 6(a) and 6(b) for $g_{AB} = 0.2$, where the populations of A and B bosons in the right well are plotted. An important difference compared to the completely imbalanced preparation is that the increase of g_A leads here to a decrease of the tunneling period T initially, reaching a minimum at $g_A \approx 0.2$. Subsequent increase of g_A leads to an increase of the period again. Resorting to the energy spectrum for an explanation [Fig. 6(c)], one should focus on the lowest doublets, which have dominant contributions from $|AA,B\rangle$ and $|B,AA\rangle$. We see a splitting of the lowest doublet as they approach the avoided crossing, leading to an increase of the tunneling rates. For larger g_A, it is the energetically excited doublets which represent the main contribution. The two levels of the excited doublet come closer in energy as g_A increases further, leading to a smaller tunneling frequency. In terms of tunneling processes, the dominant sequence here is $|AA,B\rangle \to |A,AB\rangle \to |AB,A\rangle \to |B,AA\rangle$ and a somewhat suppressed sequence is $|AA,B\rangle \to |A,AB\rangle \to |0,AAB\rangle \to |B,AA\rangle$. Using Eq. (3), the tunneling rates scale as $f \sim J^3/2g_{AB}(g_{AB} - g_A)$ for the first sequence and $f \sim J^3/(g_{AB} - g_A)^2$ for the second sequence. We see that as g_A increases from zero, the tunneling frequency increases, reaching a maximum for $g_{AB} = g_A$ (it does not actually diverge as the formula suggests since in this case other higher order

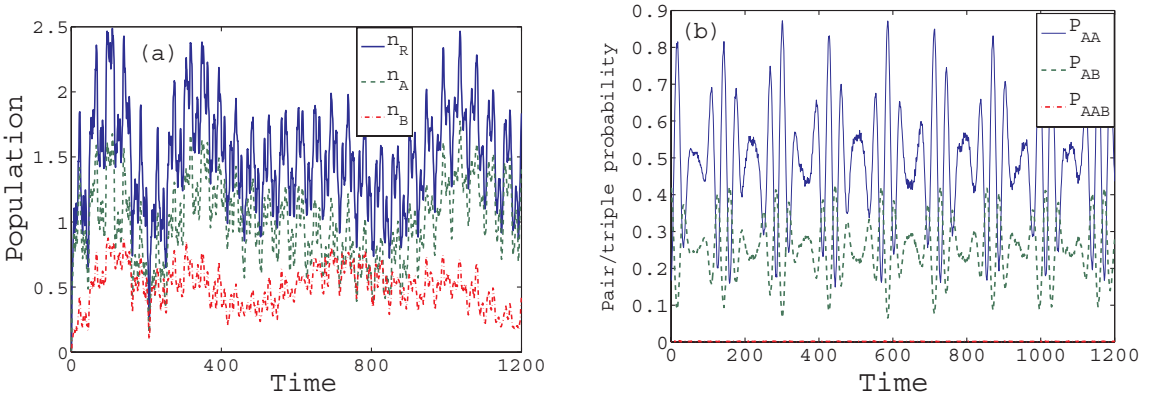

FIG. 5. (Color online) (a) Population in the right well of the total n_R and the individual species n_A, n_B for $g_{AB} = 25.0$ $g_A = 20.0$. (b) Pair and triple probability. P_{AA}, P_{AB}, and P_{AAB} correspond to the probabilities of finding AA, AB, and AAB bosons in the same well, respectively.

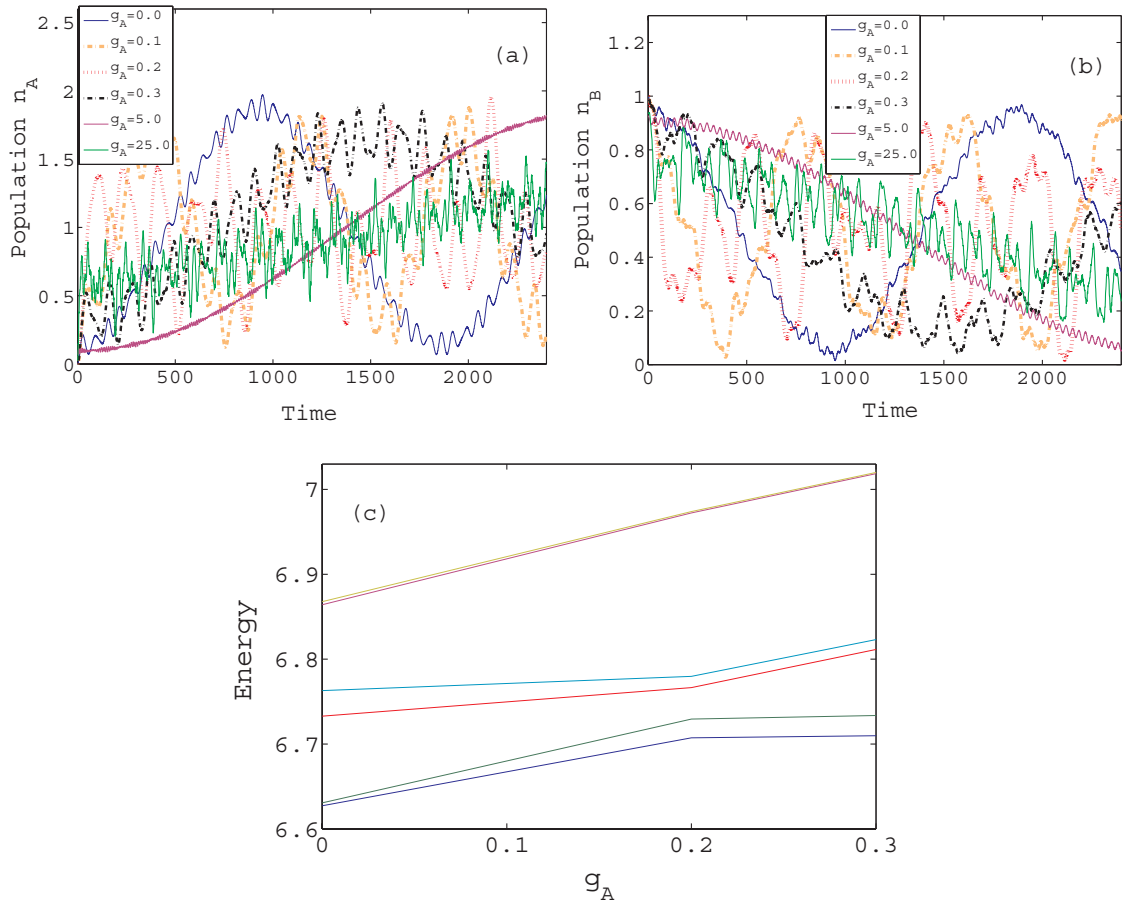

FIG. 6. (Color online) Population of the right well (a) n_A of species A and (b) n_B of species B at $g_{AB} = 0.2$ for different values of g_A for a species-separated initial state. (c) Energy spectrum for $g_{AB} = 0.2$.

terms with respect to J become relevant), while beyond this point the period increases again. The crucial difference with the previous case of a completely imbalanced initial condition is the sign in the denominator, which was positive previously and is negative here. This implies that while in previous case there was a monotonic increase in the tunneling period with increasing g_A, here we encounter an initial decrease as g_A approaches g_{AB}. For very high values $g_A = 25.0$, additional states contribute to the dynamics, leading to the high-frequency noise observed.

The avoided crossing present for the lowest lying states of the energy spectrum occurs also for higher values of g_{AB} near $g_A \approx g_{AB}$. This results in a similar dynamical behavior with respect to the dependence on g_A. The case of high interactions $g_{AB} = 25.0$, which is illustrated in Fig. 7, is different. Here the tunneling period decreases substantially as g_A takes larger values. The very smooth behavior for $g_A = 0$ [Fig. 7(a)], where in principle only the lowest doublet $|AA,B\rangle \pm |B,AA\rangle$ contributes, changes to rapid small oscillations and erratic patterns as the intraspecies interaction increases, indicating that other higher lying states are involved in the dynamics. The strong intraspecies repulsion here serves again as the principal destructor of the correlated shuffling between the initial state and its mirror number state. We can attribute the increase of the tunneling rate to the increase of the density overlaps due to intra- and interspecies strong repulsion, along the line of the arguments provided in the discussion of Fig. 4.

As a last remark on the dynamics of the species-separated initial state, we comment on the degree of correlation of the tunneling. Since the tunneling consists in principle of shuffling between $|AA,B\rangle$ and $|B,AA\rangle$, the two species spent most of the time in different wells. Therefore, the probability of finding B and A species in the same well remains always close to zero, while the A particles tunnel as a pair. As described in the previous section, this behavior ceases to exist in general for strong g_A where single-particle tunneling for the A species via excited states is induced. Note that for the cases of initial states discussed thus far, the destruction of the correlated tunneling behavior (three bosons staying together and the two species remaining separated) results from a strong increase of the intraspecies interaction, which drives the system beyond the simple number-state dynamics ($|AAB,0\rangle \Leftrightarrow |0,AAB\rangle$ or $|AA,B\rangle \Leftrightarrow |B,AA\rangle$). We show next that such strong deviations from the initial-state configuration can also be achieved for the situation of a partially population-imbalanced initial state but for a different reason.

V. PARTIAL POPULATION-IMBALANCED INITIAL STATE

A novel tunneling mechanism is encountered if the initial state is prepared such that the two wells share an equal

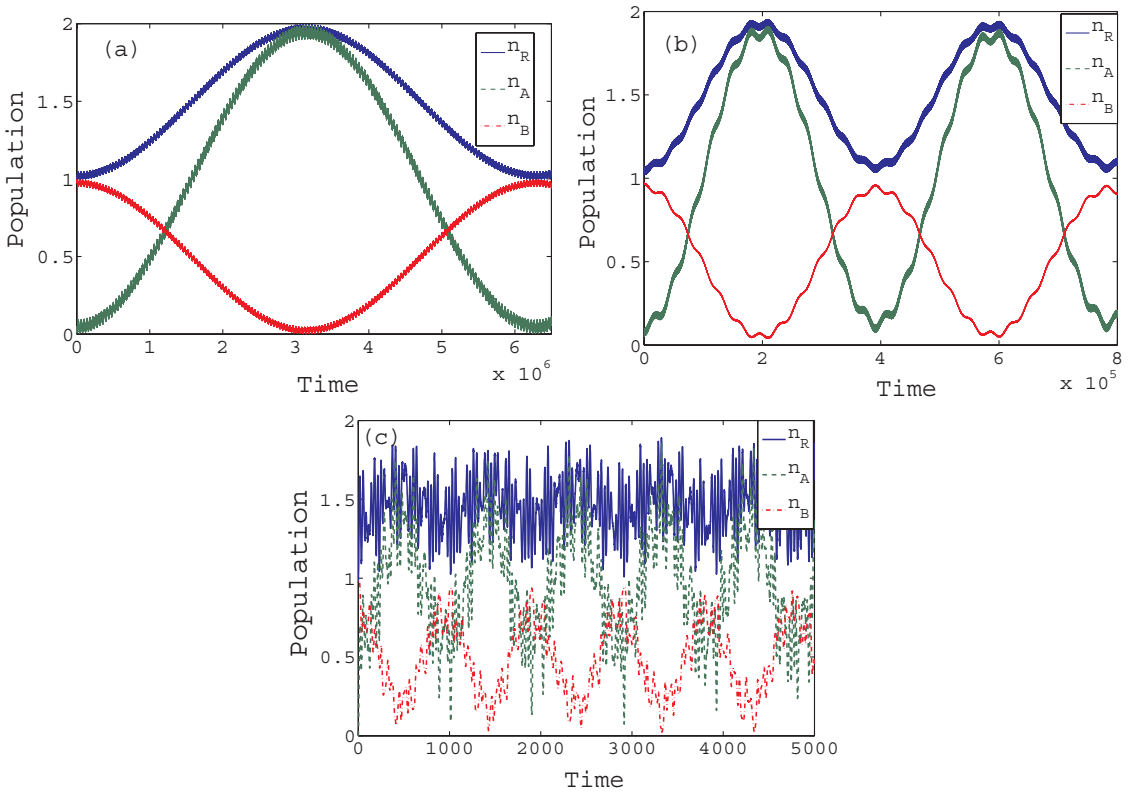

FIG. 7. (Color online) Population of the right well n_R, n_A, and n_B for $g_{AB} = 25.0$, (a) $g_A = 0.0$, (b) $g_A = 5.0$, and (c) $g_A = 20.0$ for the species-separated initial state.

mean value of the population of A atoms while the B atom is on the left well. This initial state we call *partially population-imbalanced* state. The behavior observed above, namely the increase of the tunneling period with increasing g_{AB} and its decrease with increasing g_A, can still be observed here. However, a major difference compared to the preceding cases arises in terms of the evolution of the different states, which is reflected in the corresponding time evolution of the populations.

In Fig. 8, we show the populations n_A, n_B, and n_R for $g_{AB} = 0.2$. Naively, one would expect that the the B boson will undergo Rabi oscillations on the background of the A bosons, which should remain with equal population in each well. However, this does not happen for $g_{AB} > g_A$. The envelope behavior of the A particle population [i.e., n_A in Fig. 8(a) for $g_A = 0$] first increases then decreases, indicating that the single A atom in the right well tunnels partially to the left well, thus decreasing the population of the A particles in the right well. The B boson, on the other hand, tunnels completely to the right well. This process is retained thereafter and is overall periodic. The envelope behavior is modulated by high-frequency oscillations of significant amplitude involving a rapid tunneling between the two wells. As g_A is increased from 0 to 0.2, the pattern becomes more irregular, consisting mainly of a constant envelope, and shows rapid oscillations. The amplitude of the oscillation of n_A remains large. When the intraspecies interaction strength $g_A = 0.3$ becomes larger than the interspecies coupling $g_{AB} = 0.2$ [Fig. 8(c)], the tunneling of A bosons is strongly suppressed. For even higher interactions $g_A = 5.0$ [Fig. 8(d)], the A bosons are completely localized while the B boson undergoes Rabi oscillations between the two wells, as one would expect intuitively since the highly repulsive species A are initially in different wells.

The evolution of the dynamics shows further characteristics for stronger interspecies interactions. Figure 9 presents the results for $g_{AB} = 5.0$. For $g_A = 0.0$ [Fig. 9(a)], there are two distinct oscillations for both n_A and n_B: a fast fluctuation with significant amplitude for n_B coupled to a large amplitude motion of n_A. Intuitively, one can understand this behavior (seen also in the previous case) for large g_{AB} as follows: The tunneling of the B boson to the right well pushes the A bosons to the left well due to the strong repulsion and vise versa, leading to a counterflow type of dynamics. The fast oscillation of considerable amplitude for n_A involves tunneling of a "complete" A boson and partial tunneling of a B boson between the wells. The origin of these oscillations can be understood via the number-state decomposition of the initial state, as will be explained below. In contrast, for $g_A = 4.0$ [Fig. 9(b)], the tunneling of A bosons is considerably suppressed and the B boson undergoes a rapid oscillation between the wells. For even higher g_A as before, we get an almost complete suppression of the A boson tunneling while the B boson executes the same very fast oscillations.

For very strong interspecies interaction $g_{AB} = 25.0$, a similar pattern is seen for low g_A (not shown), albeit with a much longer period. For quite strong $g_A = 5.0$, there is a tendency for suppression of the tunneling of the A boson [Fig. 9(c)], which still oscillates but with a small amplitude.

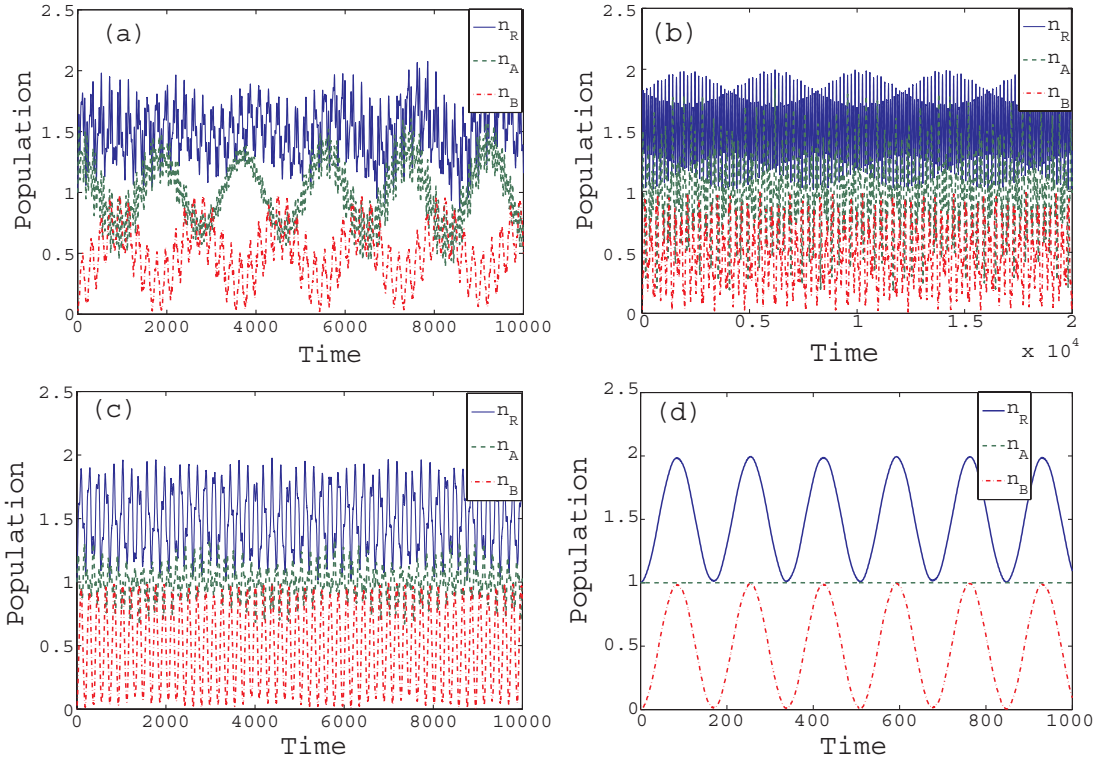

FIG. 8. (Color online) Population in the right well n_R, n_A, and n_B for $g_{AB} = 0.2$ and for (a) $g_A = 0.0$, (b) $g_A = 0.2$, (c) $g_A = 0.3$, and (d) $g_A = 5.0$.

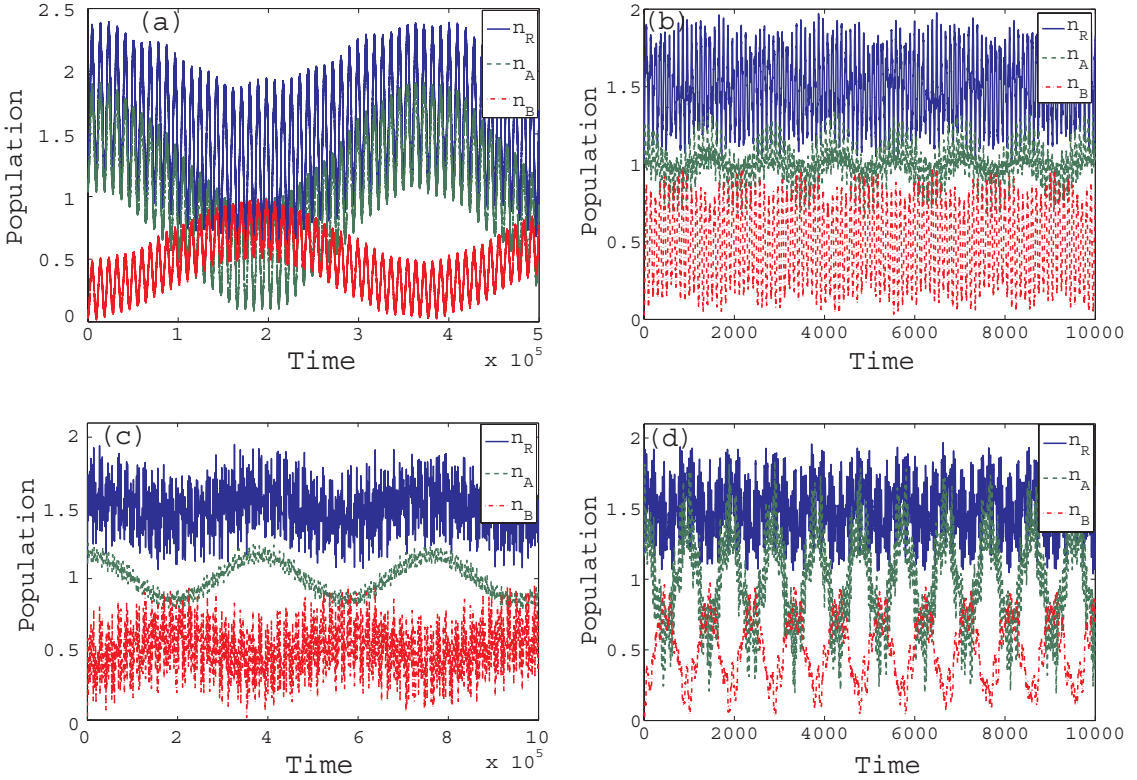

FIG. 9. (Color online) Population in the right well n_R, n_A, and n_B for (a) $g_{AB} = 5.0$ and $g_A = 0.0$, (b) $g_{AB} = 5.0$ and $g_A = 4.0$, (c) $g_{AB} = 25.0$ and $g_A = 5.0$, and (d) $g_{AB} = 25.0$ and $g_A = 20.0$.

Unlike $g_{AB} = 5.0$, increasing the interaction to $g_A = 20.0$ [Fig. 9(d)] does not reduce the tunneling of the A bosons but increases it approaching a "fermionization" type of behavior of the dynamics.

To identify the underlying dynamical mechanisms leading to the above observations, we first note that the initial state in this case is not necessarily a pure number state $|AB,A\rangle$ but is a linear combination of the number states $|AAB,0\rangle$, $|AB,A\rangle$, and $|B,AA\rangle$, maintaining the required population balance of the initial state (equal population of A bosons in each well and the B boson in the left well).

For this initial setup, the tunneling dynamics consists of transferring the atoms between the initial state and a target state composed of the number states $|0,AAB\rangle$, $|A,AB\rangle$, and $|AA,B\rangle$. For $g_{AB} \gg g_A$, the number state $|AA,B\rangle$ represents the dominant contribution to the target state and thus the dynamics consists of transferring the atoms between the initial state and the configuration $|AA,B\rangle$. As a result, we have tunneling of the B boson to the right well and of a single A boson to the left well, which we can observe in the envelope behavior of n_A and n_B of Fig. 8(a) and more prominently in Fig. 9(a). The faster oscillations are the result of the contributions from the states $|0,AAB\rangle$ and $|A,AB\rangle$. For $g_{AB} \approx g_A$, we have contributions of approximately the same magnitude from almost all the number states, leading to Josephson-like oscillations. However, for $g_{AB} \ll g_A$, the dominant contribution of the target state is $|A,AB\rangle$ and thus the system shows a transfer between the initial state and the state $|A,AB\rangle$. Therefore, the A bosons are effectively localized while the B bosons undergo Rabi oscillations between the wells.

VI. CONCLUSION AND OUTLOOK

We have investigated the tunneling dynamics of a strongly correlated few-body bosonic binary mixture in a one-dimensional double well covering the complete range of intra- and interspecies interaction. Our focus is the interplay of the inter- and intraspecies correlations and their impact on the dynamics. We observe that the tunneling period increases drastically as the interspecies interaction g_{AB} increases, which is due to quasidegenerate symmetric states contributing primarily to the dynamics. This effect is quite general and observed here for different initial configurations.

The intraspecies coupling g_A possesses a different impact on the behavior of the dynamics, depending on the strength g_{AB} as well as on the initial state. The general trend is that for large g_A the overlap of localized wave functions of contributing states becomes larger and thus the effective tunneling coupling is increased, leading to higher tunneling frequencies. For low interactions, different behavior is encountered for different setups. For a completely imbalanced initial state, for instance, we observe that for small values of g_{AB}, the tunneling period increases as we increase g_A in the weak interaction regime. However, for larger values of g_A, the tunneling period reduces with increasing g_A. This behavior is not seen for the species-separated initial condition. In the latter case, we observe a minimal period at $g_A = g_{AB}$, which is a manifestation of an avoided crossing in the spectrum.

Concerning the different initial states of the ensemble, the complete population-imbalanced state exhibits generically a completely correlated tunneling process for the A and B species, which breaks only for large values of g_A, leading to an attempted single-particle tunneling and independent fermion-like behavior. For the species-separated scenario, the two species tend to stay in opposite wells when the interspecies repulsion is large, a behavior which alters only if g_A also becomes large. For the partially population-imbalanced case where the mean population of A atoms in each well $n_A = 1$, one would intuitively expect that the A particles remain in different wells due to their initial preparation, but this happens only if the interaction between them is considerably large. In the other cases, the A particles undergo oscillations and the initially mixed state where an A and a B boson coexist in the same well can turn into a separated state for which the A and B species reside in different wells.

Understanding the fundamental effects and mechanisms of the tunneling dynamics in strongly correlated bosonic mixtures on a few-body level can be seen as a starting point to realize systems such as bosonic transistors or to create schemes for selective transport of individual bosonic component in reservoir-sink systems as well as for studies of entanglement and statistical properties of mixed ensembles. Further considerations could include higher numbers of particles or species and effects of parameters which differentiate the two species.

ACKNOWLEDGMENTS

B.C. gratefully acknowledges the financial and academic support from the International Max-Planck Research School for Quantum Dynamics in Physics, Chemistry, and Biology. L.C. gratefully thanks the Alexander von Humboldt Foundation (Germany). P.S. acknowledges financial support by the Deutsche Forschungsgemeinschaft (DFG).

APPENDIX: COMPUTATIONAL METHOD MCTDH

Our goal is to study the bosonic quantum dynamics for weak to strong interactions in a numerically exact fashion. This is computationally challenging and can be achieved only for a few-atom system. Our approach is the MCTDH method [47,48], a wave packet dynamical tool known for its outstanding efficiency in high-dimensional applications.

The principle idea is to solve the time-dependent Schrödinger equation

$$i\dot{\Psi}(t) = H\Psi(t)$$

as an initial-value problem by expanding the solution in terms of Hartree products $\Phi_J \equiv \varphi_{j_1} \otimes \cdots \otimes \varphi_{j_N}$:

$$\Psi(t) = \sum_J A_J(t)\Phi_J(t). \tag{A1}$$

The unknown single-particle functions $\varphi_j (j = 1, \ldots, n$, where n refers to the total number of single-particle functions used in the calculation) are in turn represented in a fixed primitive basis implemented on a grid. The correct bosonic permutation symmetry is obtained by symmetrization of the expansion coefficient A_J. Note that in the above expansion not only are the coefficients A_J time dependent but so are the single-particle functions φ_j. Using the Dirac-Frenkel variational principle, one can derive the equations of motion

for both A_J and Φ_J. Integrating these differential equations of motion gives us the time evolution of the system via Eq. (A1). This has the advantage that the basis $\Phi_J(t)$ is variationally optimal at each time t. Thus it can be kept relatively small, rendering the procedure more efficient.

Although MCTDH is designed primarily for time-dependent problems, it is also possible to compute stationary states. For this purpose the *relaxation* method is used [49]. The key idea is to propagate a wave function Ψ_0 by the nonunitary operator $e^{-H\tau}$. As $\tau \to \infty$, this exponentially damps out any contribution but that stemming from the true ground state like $e^{-(E_m - E_0)\tau}$. In practic,e one relies upon a more sophisticated scheme called the *improved relaxation* [50,51], which is much more robust, especially for excited states. Here $\langle\Psi|H|\Psi\rangle$ is minimized with respect to both the coefficients A_J and the orbitals φ_j. The effective eigenvalue problems thus obtained are then solved iteratively by first solving A_J with fixed orbital φ_j and then optimizing φ_j by propagating them in imaginary time over a short period. This cycle is then repeated.

We note here that the computation of very long tunneling times using the MCTDH propagation scheme is numerically impractical. For these cases, we computed the dynamics through the expansion of few-body eigenstates. Moreover, for extremely close quasidegenerate states, convergence is difficult. In these cases, a simultaneous relaxation of a whole set of these eigenstates, keeping them orthogonal, is performed by a method known as block relaxation.

[1] L. Pitaevskii and S. Stringari, *Bose-Einstein Condensation* (Oxford University Press, Oxford, 2003).

[2] C. J. Pethick and H. Smith, *Bose-Einstein Condensation in Dilute Gases* (Cambridge University Press, Cambridge, 2008).

[3] I. Bloch, J. Dalibard, and W. Zwerger, Rev. Mod. Phys. **80**, 885 (2008).

[4] I. Buluta and F. Nori, Science **326**, 108 (2009).

[5] M. Greiner *et al.*, Nature (London) **415**, 39 (2002).

[6] M. Lewenstein, A. Sanpera, D. Bogdan, A. Sen, and U. Sen, Adv. Phys. **56**, 243 (2007).

[7] E. Kierig, U. Schnorrberger, A. Schietinger, J. Tomkovic, and M. K. Oberthaler, Phys. Rev. Lett. **100**, 190405 (2008).

[8] C. Chin, R. Grimm, P. Julienne, and E. Tiesinga, Rev. Mod. Phys. **82**, 1225 (2010).

[9] M. Olshanii, Phys. Rev. Lett. **81**, 938 (1998).

[10] B. Paredes *et al.*, Nature (London) **429**, 277 (2004).

[11] T. Kinoshita, T. Wenger, and D. S. Weiss, Science **305**, 1125 (2004).

[12] M. Girardeau, J. Math. Phys. **1**, 516 (1960).

[13] C. J. Myatt, E. A. Burt, R. W. Ghrist, E. A. Cornell, and C. E. Wieman, Phys. Rev. Lett. **78**, 586 (1997).

[14] D. S. Hall, M. R. Matthews, J. R. Ensher, C. E. Wieman, and E. A. Cornell, Phys. Rev. Lett. **81**, 1539 (1998).

[15] P. Maddaloni, M. Modugno, C. Fort, F. Minardi, and M. Inguscio, Phys. Rev. Lett. **85**, 2413 (2000).

[16] G. Modugno, M. Modugno, F. Riboli, G. Roati, and M. Inguscio, Phys. Rev. Lett. **89**, 190404 (2002).

[17] J. Catani, L. DeSarlo, G. Barontini, F. Minardi, and M. Inguscio, Phys. Rev. A **77**, 011603 (2008).

[18] M. A. Cazalilla and A. F. Ho, Phys. Rev. Lett. **91**, 150403 (2003).

[19] O. E. Alon, A. I. Streltsov, and L. S. Cederbaum, Phys. Rev. Lett. **97**, 230403 (2006).

[20] T. Mishra, R. V. Pai, and B. P. Das, Phys. Rev. A **76**, 013604 (2007).

[21] T. Roscilde and J. I. Cirac, Phys. Rev. Lett. **98**, 190402 (2007).

[22] A. Kleine, C. Kollath, I. P. McCulloch, T. Giamarchi, and U. Schollwöck, Phys. Rev. A **77**, 013607 (2008).

[23] M. D. Girardeau and A. Minguzzi, Phys. Rev. Lett. **99**, 230402 (2007).

[24] S. Zöllner, H.-D. Meyer, and P. Schmelcher, Phys. Rev. A **78**, 013629 (2008).

[25] Y. Hao and S. Chen, Eur. Phys. J. D **51**, 261 (2009).

[26] Y. Hao, Y. Zhang, X.-W. Guan, and S. Chen, Phys. Rev. A **79**, 033607 (2009).

[27] E. Tempfli, S. Zöllner, and P. Schmelcher, New J. Phys. **11**, 073015 (2009).

[28] A. Hu, L. Mathey, I. Danshita, E. Tiesinga, C. J. Williams, and C. W. Clark, Phys. Rev. A **80**, 023619 (2009).

[29] A. N. Salgueiro *et al.*, Eur. Phys. J. D **44**, 537 (2007).

[30] D. R. Dounas-Frazer, A. M. Hermundstad, and L. D. Carr, Phys. Rev. Lett. **99**, 200402 (2007).

[31] L. Wang, Y. Hao, and S. Chen, Eur. Phys. J. D **48**, 229 (2008).

[32] S. Zöllner, H.-D. Meyer, and P. Schmelcher, Phys. Rev. Lett. **100**, 040401 (2008).

[33] S. Zöllner, H.-D. Meyer, and P. Schmelcher, Phys. Rev. A **78**, 013621 (2008).

[34] M. Albiez, R. Gati, J. Fölling, S. Hunsmann, M. Cristiani, and M. K. Oberthaler, Phys. Rev. Lett. **95**, 010402 (2005).

[35] T. Anker, M. Albiez, R. Gati, S. Hunsmann, B. Eiermann, A. Trombettoni, and M. K. Oberthaler, Phys. Rev. Lett. **94**, 020403 (2005).

[36] L.-M. Kuang and Z.-W. Ouyang, Phys. Rev. A **61**, 023604 (2000).

[37] X. Q. Xu, L. H. Lu, and Y. Q. Li, Phys. Rev. A **78**, 043609 (2008).

[38] G. Mazzarella, M. Moratti, L. Salasnich, M. Salerno, and F. Toigo, J. Phys. B **42**, 125301 (2009).

[39] I. I. Satija, R. Balakrishnan, P. Naudus, J. Heward, M. Edwards, and C. W. Clark, Phys. Rev. A **79**, 033616 (2009).

[40] B. Julia-Diaz, M. Guilleumas, M. Lewenstein, A. Polls, and A. Sanpera, Phys. Rev. A **80**, 023616 (2009).

[41] B. Sun and M. S. Pindzola, Phys. Rev. A **80**, 033616 (2009).

[42] A. Naddeo and R. Citro, J. Phys. B **43**, 135302 (2010).

[43] A. Hu, L. Mathey, E. Tiesinga, I. Danshita, C. J. Williams, and C. W. Clark, Phys. Rev. A **84**, 041609(R) (2011).

[44] A. C. Pflanzer, S. Zöllner, and P. Schmelcher, J. Phys. B: At., Mol. Opt. Phys. **42**, 231002 (2009).

[45] A. C. Pflanzer, S. Zöllner, and P. Schmelcher, Phys. Rev. A **81**, 023612 (2010).

[46] A. Widera, W. Alt, and D. Meschede, J. Phys.: Conf. Ser. **264**, 012021 (2011).

[47] H.-D. Meyer, U. Manthe, and L. S. Cederbaum, Chem. Phys. Lett. **165**, 73 (1990).

[48] M. H. Beck, A. Jäckle, G. A. Worth, and H.-D. Meyer, Phys. Rep. **324**, 1 (2000).

[49] R. Kosloff and H. Tal-Ezer, Chem. Phys. Lett. **127**, 223 (1986).

[50] H.-D. Meyer and G. A. Worth, Theor. Chem. Acc. **109**, 251 (2003).

[51] H.-D. Meyer, F. L. Quéré, C. Léonard, and F. Gatti, Chem. Phys. **329**, 179 (2006).